Electronic Supplementary Information (ESI):

Sustainable Release of $Mg(NO_3)_2$ from Separator Boosts Electrochemical Performance of Lithium Metal as Anodes for Secondary Batteries

Shuang Xia [a], Zhifeng Lin[a], Bohao Peng [a], Xuelong Yuan [a], Jingzhen Du [a], Xinhai Yuan [a], Lili Liu [a,*], Lijun Fu [a], Rudolf Holze [b,c], Yuping Wu [a,b,*]

[a] State Key Laboratory of Materials-oriented Chemical Engineering & School of Energy Science and Engineering, Nanjing Tech University, Nanjing 211816, China

[b] Confucius Energy Storage Lab, School of Energy and Environment & Z Energy Storage Center, South East University, Nanjing 210096, China

[c] Chemnitz University of Technology, D-09107 Chemnitz, Germany;

Experimental Procedures

Materials

All solvents and reagents obtained from commercial sources were used without further purification. Base separators (DKJ-14) were purchased from Zhejiang DKJ New Energy Tech Co., Ltd. The LS-009 (1.0 M LiTFSI imide in DOL/ DME =1: 1 Vol% with 2.0 wt% $LiNO_3$) and LB-315 (1M $LiPF_6$ in DMC/ EC/ EMC=1: 1: 1 Vol%) electrolyts were obtained from DodoChem Co., Ltd (LiTFSI: lithium bis(trifluoromethanesulfonyl)imide, DOL: 1,3-Dioxolane, DME: 1,2-dimethoxyethane, DMC: dimethyl carbonate, EC: ethylene carbonate, EMC: ethyl methyl carbonate). The carbon-coated Al foil and carbon papers were purchased from Guangdong Canrd New Energy Technology Co., Ltd. Magnesium nitrate hexahydrate ($Mg(NO_3)_2$•$6H_2O$, MNH), Super P, DME, polyvinylidene difluoride (PVDF), sublimated sulfur (S), carbon black (CB), carbon nanotubes (CNTs), *N*-methyl pyrrolidone (NMP), *N,N*-dimethylformamide (DMF), carboxymethyl cellulose (CMC), and ferrous lithium phosphate ($LiFePO_4$, LFP) were purchased from Shanghai Aladdin Biochemical Technology Co., Ltd.

Characterization and instruments

The morphology and structure were observed by a scanning electron microscope (Phenom ProX, SEM). The Energy-dispersive X-ray spectroscopy (EDS) was taken at 15 kV. X-ray Diffraction (XRD, Smart Lab3KW) was used from 10-90°with Cu Kα radiation at the scanning rate of $10°min^{-1}$. The contact angles were recorded by a contact angle meter (Kino).

Electrochemical measurements

The cycling and rate performance of the batteries were tested by the battery test system (LAND CT2001A, Wuhan, China). Electrochemical impedance spectra (EIS, 10^{-2}~10^{5} Hz) and Cyclic voltammetry (CV) were tested by electrochemical workstation (Chenhua, CHI760e).

Calculation

According to equation (1), the ionic conductivity of prepared separators at different temperatures can be calculated from the EIS.

$$\sigma = L / (R_b \times A) \quad \text{(S1)}$$

Here, σ is the ionic conductivity, L is the thickness of separators, R_b is the bulk resistance, and A is the contact area between the stainless steel sheet and the separator.

The activation energy of the separators can be calculated according to the Arrhenius equation (2).

$$\sigma = A \exp(-E_a / RT) \quad \text{(S2)}$$

The symbols in the equation are the pre-exponential factor (A), activation energy (E_a), and the perfect gas constant (R).

According to the Randles Sevcik equation (3), the Li^+ diffusion coefficients of cells with different separators can be calculated.

$$I_P = 2.69\times10^5 n^{1.5} A D_{Li^+}^{0.5} C_{Li} V^{0.5} \quad \text{(S3)}$$

The symbols in the equation are the peak current (Ip), the number of electron transfers during the deintercalation of lithium (n), the contact area between active substance and electrolyte (A), the Li^+ diffusion coefficient (D_{Li+}), the concentration of

Li^+ in an electrolyte (C_{Li}), and the scanning speed (V).

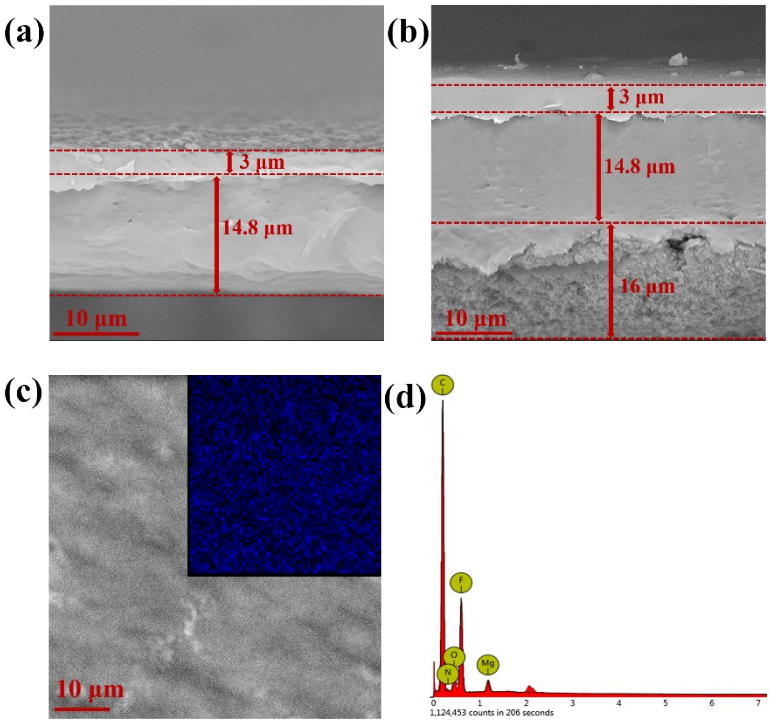

Fig. S1. Characterization of modified separators. The section SEM images of the (a) MND, (b) SP@MND. (c) EDS elemental mapping image (Mg) of the MN modified layer and (d) the corresponding EDS spectrum.

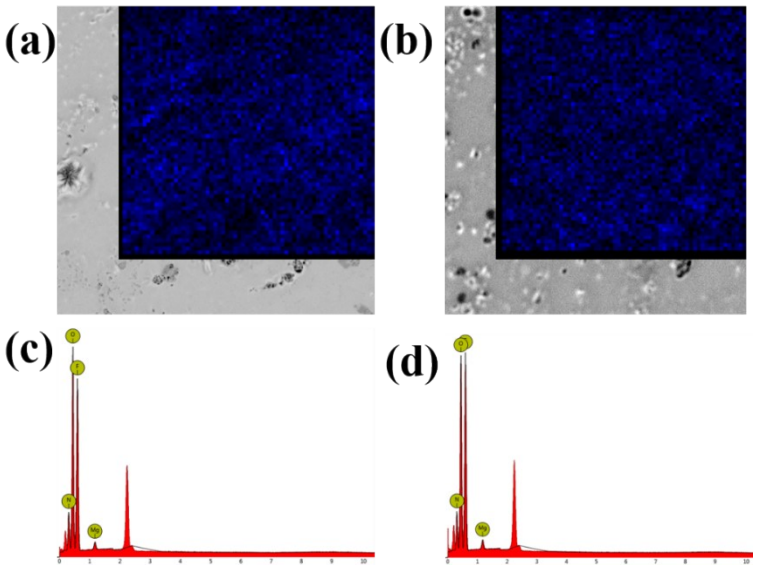

Fig. S2. EDS elemental mapping image (Mg) of the stripping Li metals after (a) 0.5 h and (b) 1 h in Li//Cu cells with the MND, and (c) (d) the corresponding EDS spectrum.

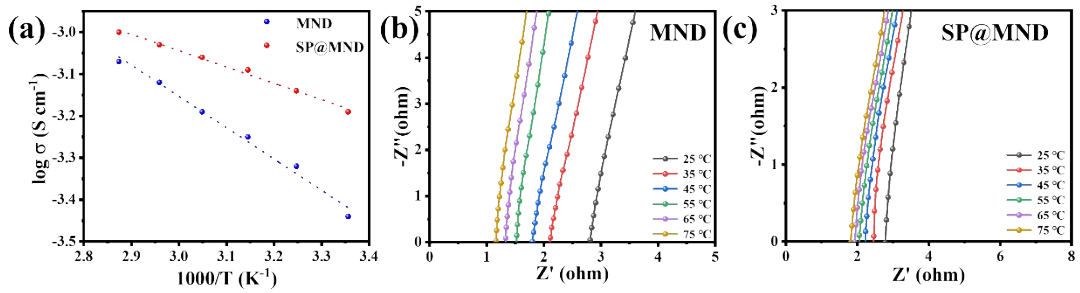

Fig. S3. (a) The Arrhenius plots of modified separators and corresponding EIS plots of the (b) MND and (c) SP@MND.

Table S1. The ICP-OES results of the SP@MND immersion in different electrolytes for 0.5 and 4 h (After immersing for 0.5 h).

Simple	LS-009 0.5 h	LB-315 0.5 h	LS-009 4 h	LB-315 4 h
Concentration of Mg (mg/L)	16.5	15.1	14.3	13.7

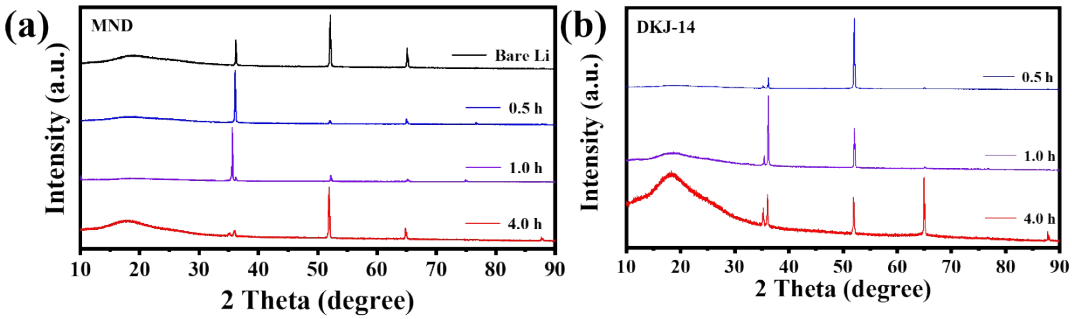

Fig. S4. XRD of Li anodes with (a) MND and (b) DKJ-14 of Li plating/stripping at 0.5 mA cm^{-2} after different stripping times.

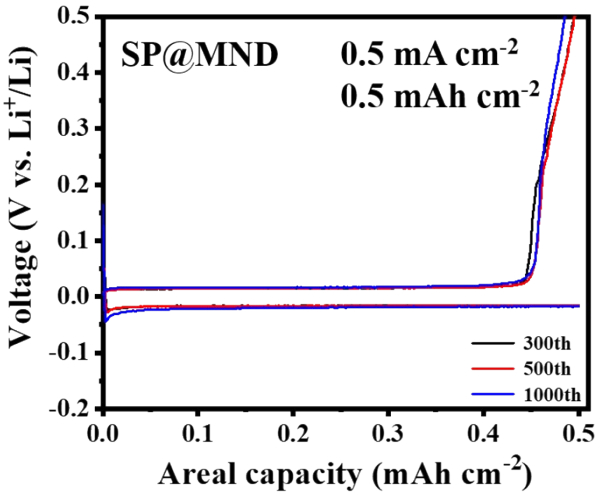

Fig. S5. Charge/discharge voltage-capacity profiles of the Li//Cu cell with the SP@MND at 0.5 mA cm^{-2}.

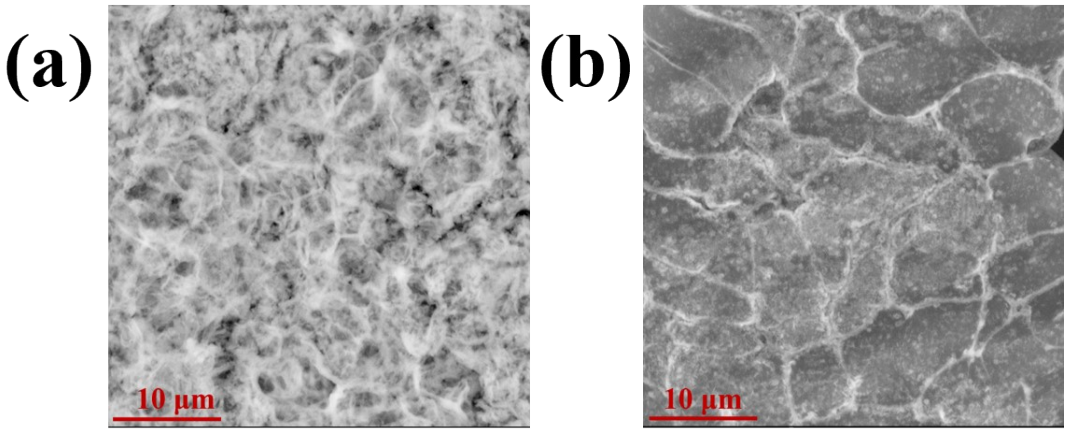

Fig. S6. SEM images of Cu electrodes with (a) DKJ-14 and (b) MND of Li plating/stripping at 0.5 mA cm^{-2} and 0.5 mAh cm^{-2} after 30 cycles.

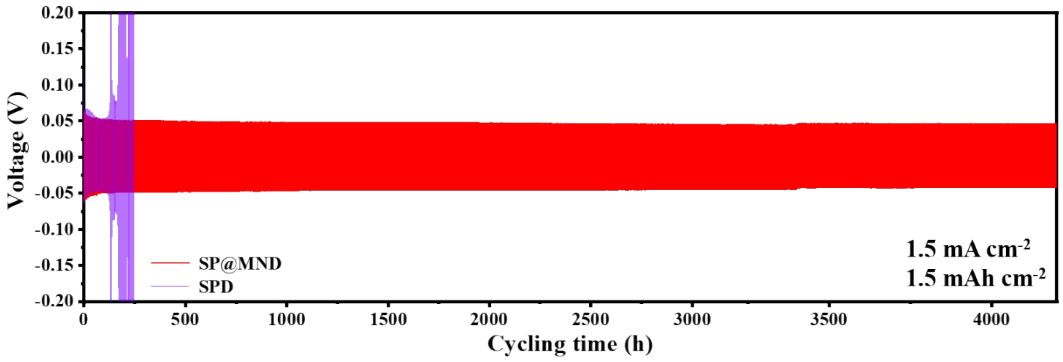

Fig. S7. The cycling performance of the Li//Li cell with the SP@MND at 1.5 mA cm^{-2} and 1.5

mAh cm^{-2}.

Table S2. A comparison of electrochemical performance in Li//Li cells with the SP@MND and other recent reports.

Separator	Electrolyte	Current Densities	Cycling Tine (h)	Ref.
SP@MND	**LS-009**	**0.5 mA cm^{-2}** **1.5 mA cm^{-2}**	**4800 h** **4200 h**	**This work**
MAF-6/PP	A	0.5 mA cm^{-2} 1.0 mA cm^{-2}	2200 h 600 h	1[1]
SCOF-2	B	1.0 mA cm^{-2}	350 h	2[2]
composite separator	LS-009	1.0 mA cm^{-2}	1200 h	3[3]
Zr-MOCN @PP	C	1.0 mA cm^{-2}	2000 h	4[4]
ANFM	D	1.0 mA cm^{-2} 2.0 mA cm^{-2}	Over 250 h 250 h	5[5]
EC	E	1.0 mA cm^{-2}	700 h	6[6]
MXene/PP/Cu-TCPP	LS-009	0.5 mA cm^{-2}	Over 300 h	7[7]
Li-Mg/LLZNO-PP/Li-Mg	LS-009	0.2 mA cm^{-2}	Over 5300 h	8[8]
SPLTOPD	LS-009	0.5 mA cm^{-2}	Over 1800 h	9[9]

Note: A: 1 M LiTFSI in DOL/DME=1:1,v/v+1 wt% $LiNO_3$, B: 1M LiTFSI dissolved in a mixture of DOL and DME (1:1 by volume) with 0.1 M $LiNO_3$ additive, C: 1.0 M LiPF6 in EC/DMC/EMC (by weight) and 1 wt% of VC, D: 1 mol/L $LiCF_3SO_3$ DOL: DME (v/v = 1/1), E: 1M $LiPF_6$ in EC/DEC = 1/1 (v/v) with 10 wt.% FEC additive.

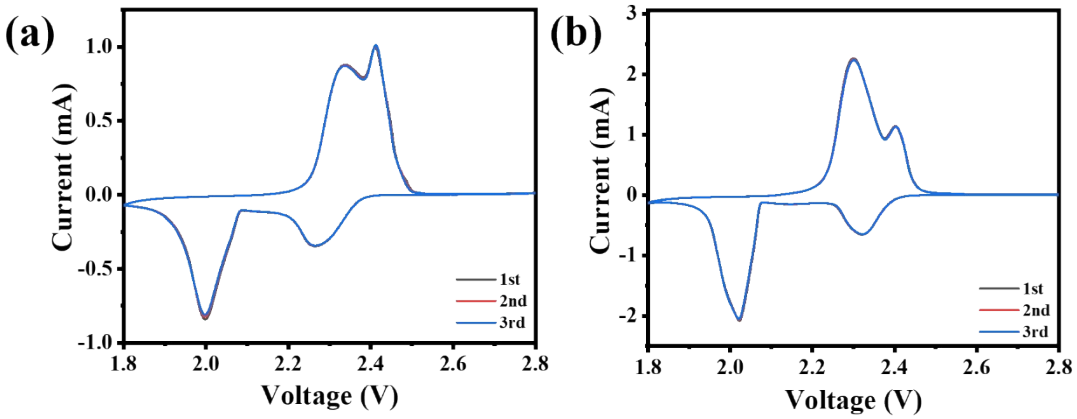

Fig. S8. The CV curves of Li//S cells with (a) the MND and (b) SP@MND at 0.1 mV s^{-1}.

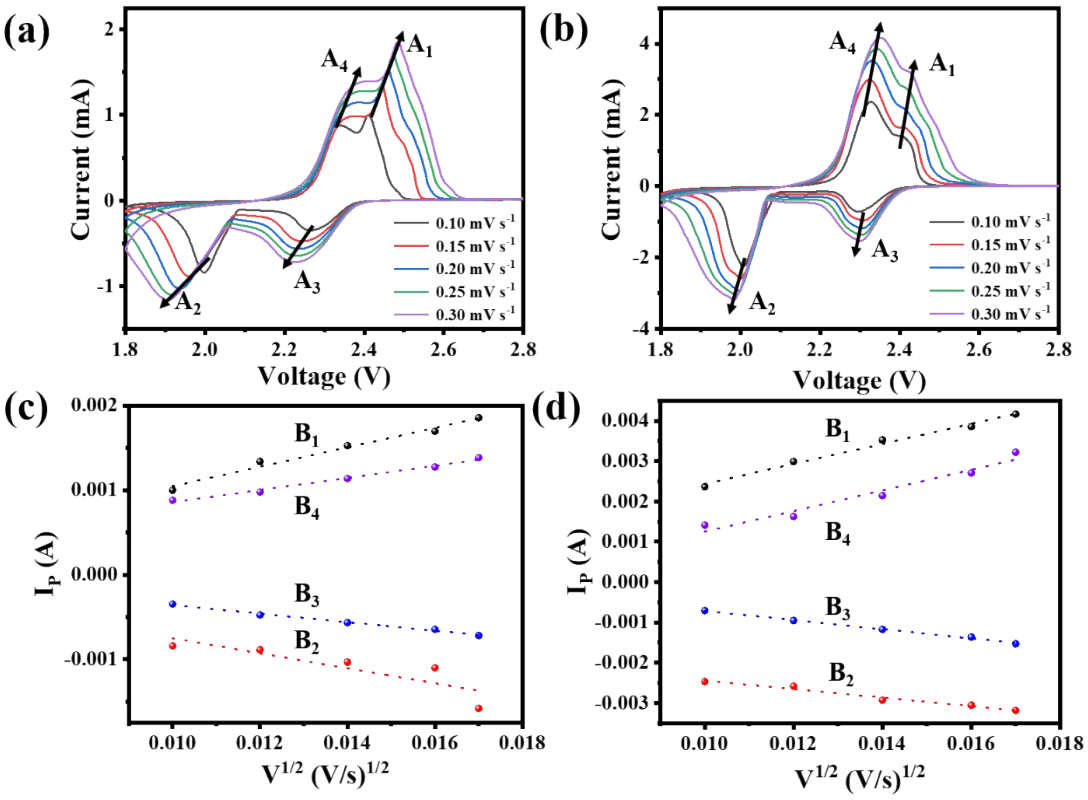

Fig. S9. The CV tests of the Li//S batteries with the (a) MND and (b) SP@MND at different scan rates and (c) (d) the corresponding linear matching of peak currents.

Table S3. Li^+ diffusion coefficients.

Separators	D_{Li^+}(cm^2/s)-anodic peak around 2.5 V	D_{Li^+}(cm^2/s)-anodic peak around 2.3 V	D_{Li^+}(cm^2/s)-cathodic peak around 2.0 V	D_{Li^+}(cm^2/s)-cathodic peak around 2.3 V
MND	1.4×10^{-8}	5.5×10^{-9}	8.3×10^{-9}	2.7×10^{-9}
SP@MND	7.0×10^{-8}	6.6×10^{-8}	1.2×10^{-8}	1.4×10^{-8}

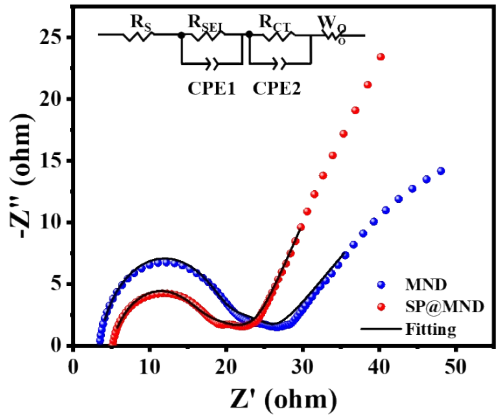

Fig. S10. EIS plots of Li//S cells with modified separators after 20 cycles at 1 C (insets: equivalent circuits).

Table S4. EIS parameters of the equivalent circuit simulation.

Cycle number	Resistance (Ω)	MND	SP@MND
After 20 cycles	R_S	3.4	4.9
	R_{SEI}	7.5	5.0
	R_{CT}	14.8	10.5

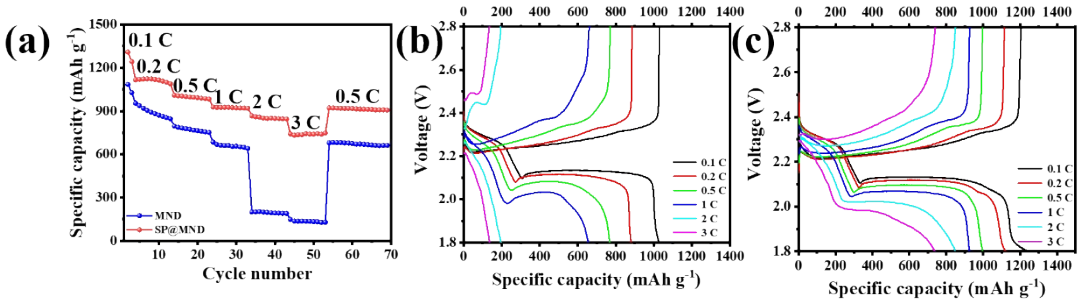

Fig. S11. Rate performance of Li//S batteries with the MND and SP@MND and the corresponding charge/discharge voltage profiles.

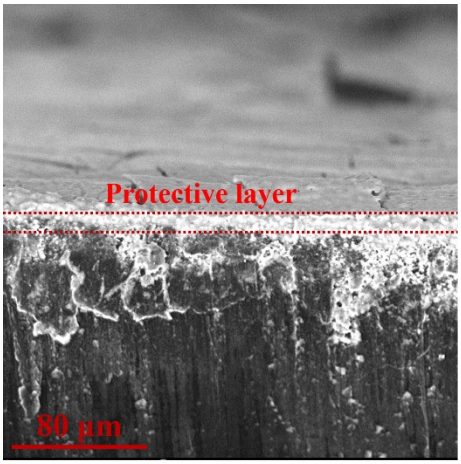

Fig. S12. SEM of Li anodes in Li//S batteries with the SP@MND after 100 cycles at 1 C.

Table S5. EDS results of the after-cycling Li anode.

Element Number	Element Symbol	Element Name	Atomic Conc.	Weight Conc.
9	F	Fluorine	46.1	51.2
8	O	Oxygen	40.8	38.2
7	N	Nitrogen	13.1	10.7

Table S6. A comparison of cycling performance of the Li//S battery with the SP@MND and other relevant reports (1 C=1675 mA g^{-1}).

Cathode	Separator	S loading (mg cm^{-2})	Cycle number	Decay rate per cycle (%)	Ref.
S/CNT	**SP@MND**	**~1.0**	**1000 (1 C)** **1000 (3 C)**	**0.060** **0.059**	**This work**
S/GO	Asy-PP/Li-Mg	1.0-1.3	400 (1 C)	0.07	1[8]
S/CNT	SPLFPPD	~1.0	800 (1 C)	0.062	2[10]
S/C	SrF_2-G/PP	NA	300 (0.5 C)	0.07	3[11]
S/C	VN_{1-x}@V-NC@PP	1.5	500 (2 C)	0.071	4[12]
S/C	Fe/Co-N-HPC /PP	2.1	300 (1 C)	0.109	5[13]
S/KB	MWCNTs/NCQ Ds/PP	1.3-1.5	500 (0.5 C)	0.1	6[14]
S/super P	SCOF	1.0	600 (1 C)	0.07	7[15]
S/super P	PyBBT-COF	1.0	100 (0.2 C)	0.27	8[16]
NA	PCA-TO@PP	0.8	200 (1 C)	0.19	9[17]
S/MWCNT	CNF/Co-Co_9S_8-NC	1.5	300 (2 C)	0.083	10[18]
S/CNT	SPLTOPD	~1.0	800 (1 C)	0.067	11[9]
S/CNT	Ni-Cu@C/HC-PP	NA	500 (0.5 C)	0.088	12[19]
CNT/S	NbB_2/rGO/PP	NA	100 (1 C)	0.27	13[20]
S/AB	w-PBDT	~1.0	500 (0.5 C)	0.088	14[21]

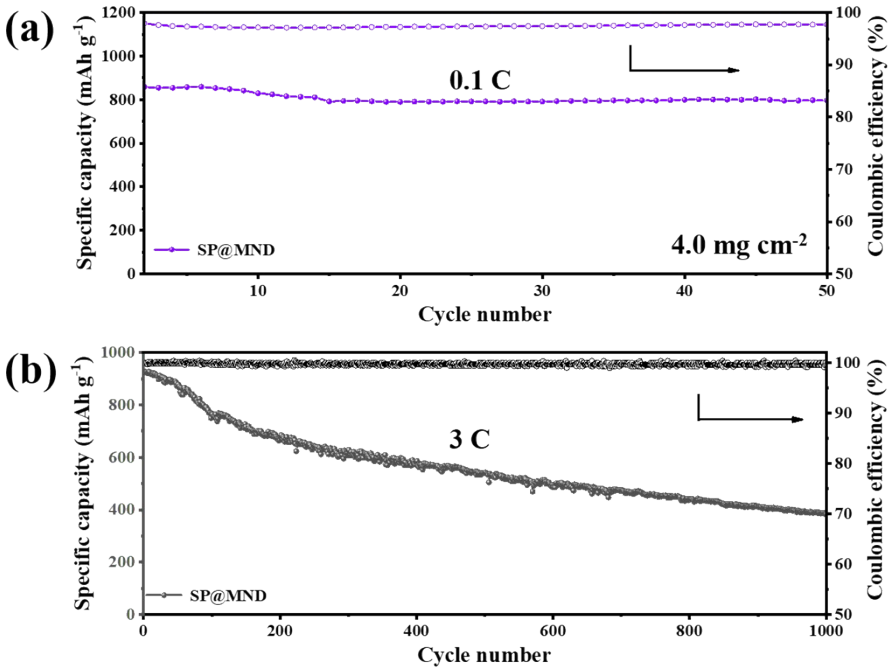

Fig. S13. Cycling performance of the Li//S batteries with the SP@MND. (a) The areal sulfur-loading is 4.0 mg cm^{-2}, and (b) cycling performance at 3 C.

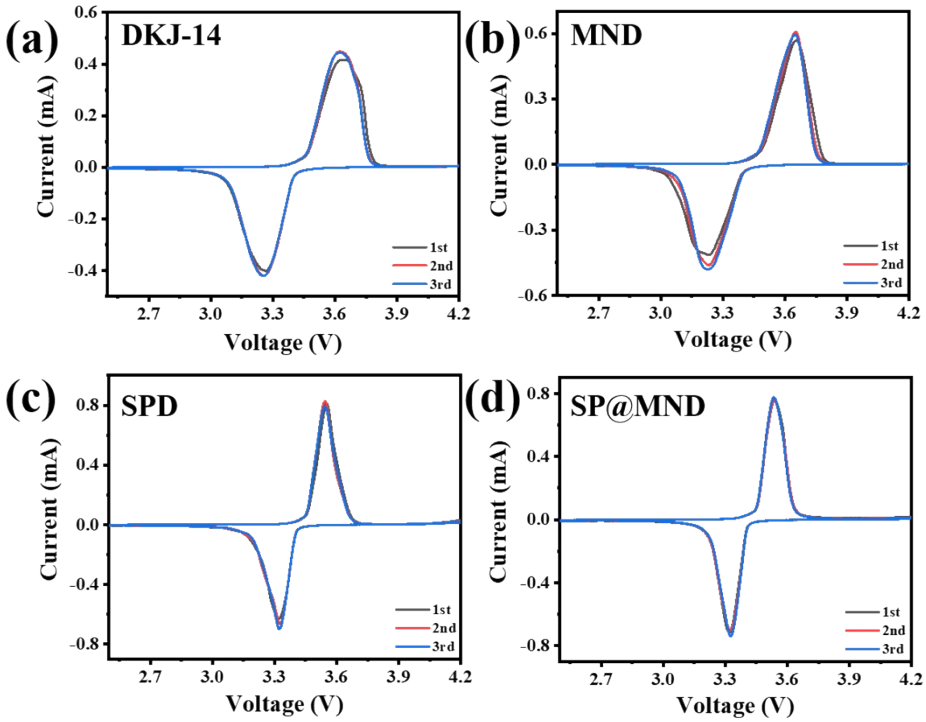

Fig. S14. The CV curves (first three cycles) of the Li//LFP batteries with the (a) DKJ-14, (b) MND, (c) SPD, and (d) SP@MND at 0.1 mV s^{-1}.

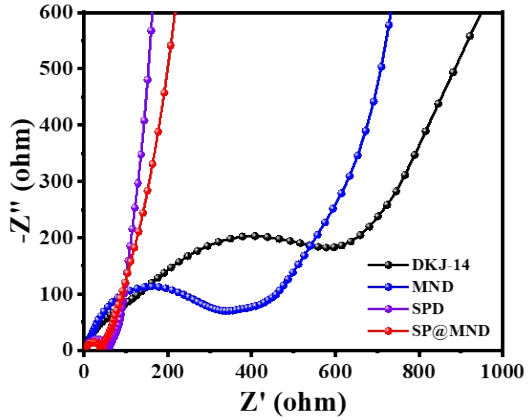

Fig. S15. The EIS tests of Li//LFP batteries with different separators.

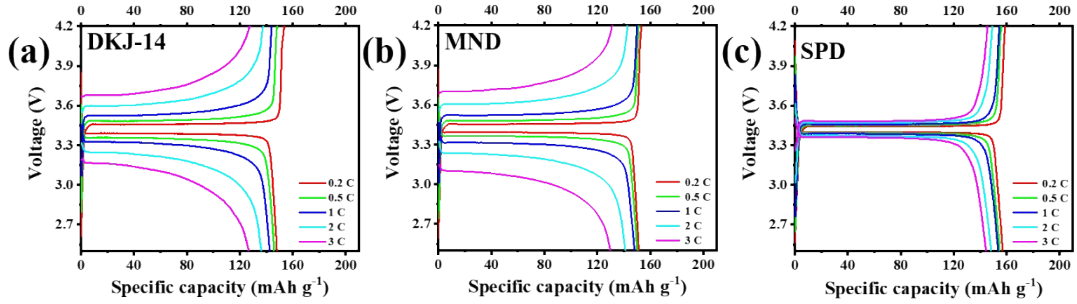

Fig. S16. Charge/discharge voltage profiles of the Li//LFP batteries with the (a) DKJ-14, (b) MND, and (c) SPD at various current densities.

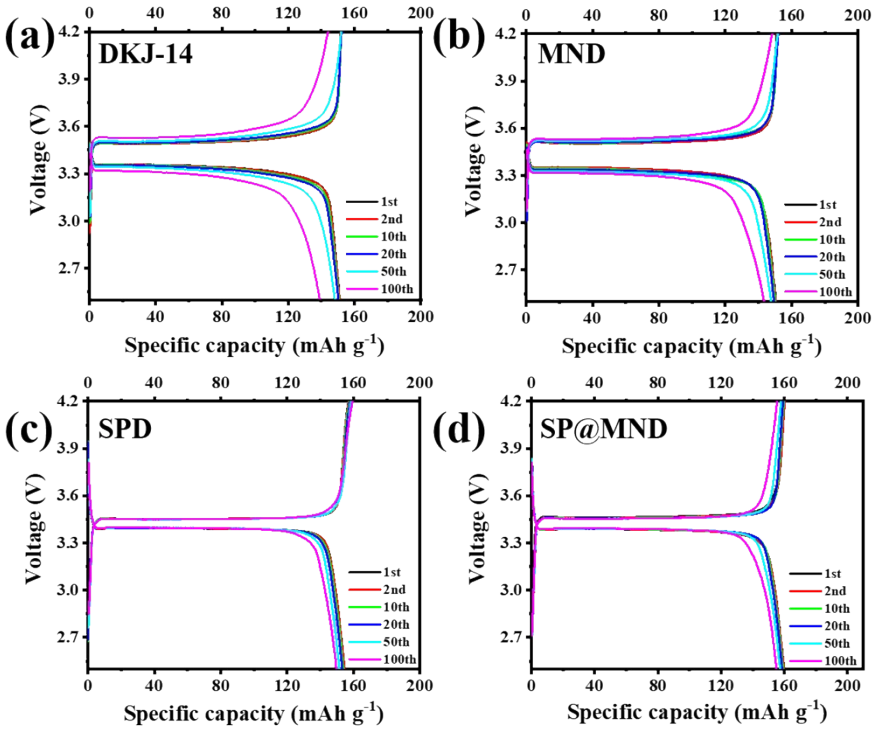

Fig. S17. Charge/discharge voltage profiles of the Li//LFP batteries with the (a) DKJ-14, (b) MND, (c) SPD and (d) SP@MND at 1 C during aging.

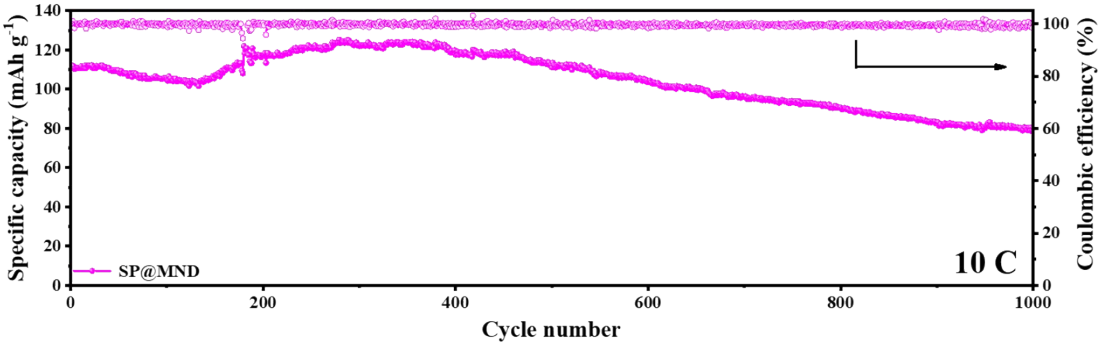

Fig. S18. Long cycling performances and coulombic efficiencies of the battery with the SP@MND at 10 C.

Table S7. A comparison of cycling performance of the Li//LFP battery with the SP@MND and other relevant reports (1 C=170 mA g^{-1}).

Separator	LFP cathode loading (mg cm^{-2})	Cycling performances	Ref.
SP@MND	**1.9(80 wt% LFP)**	**800 (1 C)** **300 (N/P=5, 1 C)** **1000 (10 C)**	**This work**
DLC/PP	1.5	1000 (5 C)	1[22]
MOFs/NA/MOFs	4.8(LFP/Graphite)	240 (0.5 C)	2[23]
f-PTC	1.75 mAh cm^{-2}	100 (1 C)	3[24]
TV-PE	NA	400 (1 C)	4[25]
PPFPA-g-Celgard	~3.0	500 (0.5 C)	5[26]
ENS	2.0	300 (1 C)	6[27]
COF-CI@PP	NA	450 (1 C)	7[28]

References

[1] W.-L. Wu, Y.-T. Xu, X. Ke, Y.-M. Chen, Y.-F. Cheng, G.-D. Lin, M.-P. Fan, L.-Y. Liu, Z.-C. Shi, *Energy Storage Materials*, 2021, **37**, 387-395.

[2] J. Xu, S. An, X. Song, Y. Cao, N. Wang, X. Qiu, Y. Zhang, J. Chen, X. Duan, J. Huang, W. Li, Y. Wang, *Advanced Materials*, 2021, **33**, 2105178.

[3] D. Han, X. Wang, Y. N. Zhou, J. Zhang, Z. Liu, Z. Xiao, J. Zhou, Z. Wang, J. Zheng, Z. Jia, B. Tian, J. Xie, Z. Liu, W. Tang, *Advanced Energy Materials*, 2022, **12**, 2201190.

[4] L. Sheng, Q. Wang, X. Liu, H. Cui, X. Wang, Y. Xu, Z. Li, L. Wang, Z. Chen, G. L. Xu, J. Wang, Y. Tang, K. Amine, H. Xu, X. He, *Nature Communications*, 2022, **13**, 172.

[5] M. Wang, A. E. Emre, J. Y. Kim, Y. Huang, L. Liu, V. Cecen, Y. Huang, N. A. Kotov, *Nature Communications*, 2022, **13**, 278.

[6] J.-Y. Seo, Y.-H. Lee, J.-H. Kim, Y.-K. Hong, W. Chen, Y.-G. Lee, S.-Y. Lee, *Energy Storage*

Materials, 2022, **50**, 783-791.

[7] Y.-H. Liu, L.-X. Li, A.-Y. Wen, F.-F. Cao, H. Ye, *Energy Storage Materials*, 2023, **55**, 652-659.

[8] W. Yan, J. L. Yang, X. Xiong, L. Fu, Y. Chen, Z. Wang, Y. Zhu, J. W. Zhao, T. Wang, Y. Wu, *Advanced Science (Weinh)*, 2022, **9**, 2202204.

[9] S. Xia, J. Song, Q. Zhou, L. Liu, J. Ye, T. Wang, Y. Chen, Y. Liu, Y. Wu, T. van Ree, *Advanced Science (Weinh)*, 2023, **10**, 2301386.

[10] S. Xia, Z. Chen, L. Yuan, J. Song, Q. Zhou, X. Yuan, L. Liu, L. Fu, Y. Chen, Y. Wu, *Journal of Materials Chemistry A*, 2023, **11**, 19870–19876.

[11] W. Jing, J. Zu, K. Zou, X. Dai, Y. Song, J. Han, J. Sun, Q. Tan, Y. Chen, Y. Liu, *Journal of Materials Chemistry A*, 2022, **10**, 4833-4844.

[12] Y. Zhang, C. Ma, C. Zhang, L. Ma, S. Zhang, Q. Huang, C. Liang, L. Chen, L. Zhou, W. Wei, *Chemical Engineering Journal*, 2023, **452**, 139410.

[13] L. Ma, J. Qian, Y. Li, Y. Cheng, S. Wang, Z. Wang, C. Peng, K. Wu, J. Xu, I. Manke, C. Yang, P. Adelhelm, R. Chen, *Advanced Functional Materials*, 2022, **32**, 2208666.

[14] Y. Pang, J. Wei, Y. Wang, Y. Xia, *Advanced Energy Materials*, 2018, **8**, 1702288.

[15] X. Deng, Y. Li, L. Li, S. Qiao, D. Lei, X. Shi, F. Zhang, *Nanotechnology*, 2021, **32**, 275708.

[16] R. Wang, Q. Cai, Y. Zhu, Z. Mi, W. Weng, Y. Liu, J. Wan, J. Hu, C. Wang, D. Yang, J. Guo, *Chemistry of Materials*, 2021, **33**, 3566-3574.

[17] C. Shi, J. Huang, Y. Tang, Z. Cen, Z. Wang, S. Liu, R. Fu, *Carbon*, 2023, **202**, 59-65.

[18] N. Gao, X. Shen, Y. Liu, Z. Xu, X. Wang, H. Liu, Y. Ren, S. Chen, Z. Li, *Journal of Materials Chemistry A*, 2023, **11**, 5212-5221.

[19] B. Zhang, J. Qie, W. Wang, Y. Li, Y. Cao, Y. Mao, J. You, C. Li, Z. Xu, *Chemical Engineering Journal*, 2024, **480**, 148022.

[20] Y. Li, Z.Wang, H. Gu,H. Jia, Z. Long, X.Yan, *ACS Nano*, 2024, **18**, 8863-8875.

[21] X. Miao, C. Song, W. Hu, Y. Ren, Y. Shen, C. Nan, *Advanced Materials*, 2024, 2401473.

[22] Z. Li, M. Peng, X. Zhou, K. Shin, S. Tunmee, X. Zhang, C. Xie, H. Saitoh, Y. Zheng, Z. Zhou, Y. Tang, *Advanced Materials*, 2021, **33**, 2100793.

[23] G. Lin, K. Jia, Z. Bai, C. Liu, S. Liu, Y. Huang, X. Liu, *Advanced Functional Materials*, 2022, **32**, 2207969.

[24] J. Ryu, D.-Y. Han, D. Hong, S. Park, *Energy Storage Materials*, 2022, **45**, 941-951.

[25] Q. Zhao, R. Wang, X. Hu, Y. Wang, G. Lu, Z. Yang, Q. Liu, X. Yang, F. Pan, C. Xu, *Advanced Science*, 2022, **9**, 2102215.

[26] S. Zheng, L. Mo, K. Chen, A. L. Chen, X. Zhang, X. Fan, F. Lai, Q. Wei, Y. E. Miao, T. Liu, Y. Yu, *Advanced Functional Materials*, 2022, **32**, 2201430.

[27] Z. Hao, C. Wang, Y. Wu, Q. Zhang, H. Xu, Y. Jin, J. Liu, H. Wang, X. He, *Advanced Energy Materials*, 2023, **13**, 2204007.

[28] S. Yao, Y. Yang, Z. Liang, J. Chen, J. Ding, F. Li, J. Liu, L. Xi, M. Zhu, J. Liu, *Advanced Functional Materials*, 2023, **33**, 2212466.